Oxford Economic Papers, 2022, 1–20
https://doi.org/10.1093/oep/gpac031

OXFORD

COVID-19 anti-contagion policies and economic support measures in the USA

Theologos Dergiades[a], Costas Milas[b]*, Elias Mossialos [c], and Theodore Panagiotidis[d]

[a]Department of International and European Studies, University of Macedonia, Thessaloniki 54636, Greece
[b]Management School, University of Liverpool, Liverpool L69 7ZH, UK
[c]Department of Health Policy, London School of Economics and Political Science, WC2A 2AE London, UK
[d]Department of Economics, University of Macedonia, Thessaloniki 54636, Greece

*Corresponding author: costas.milas@liverpool.ac.uk

Abstract

Current literature assumes that non-pharmaceutical interventions (NPIs) reduce COVID-19 infections uniformly, that is, irrespectively of their strength. The role of economic support measures (ESM) in controlling the virus is also overlooked. Using a panel threshold model of COVID-19 cases in the US states, we identify three distinct regimes of 'low', 'medium', and 'high' severity interventions; the latter being more effective towards reducing infections growth. ESM increase the efficacy of NPIs through a behavioural channel that lowers the workplace hours supplied by individuals. Nonetheless, when containment policies are not very stringent ('low' regime) or are too draconian ('high' regime), ESM are less effective towards suppressing the pandemic. Finally, we find that the largest impact towards reducing the growth of infections comes jointly from school closures, workplace closures, cancelation of public events, and restrictions on internal movement, followed by the stay-at-home requirements, and the closure of public transport.

JEL classification: H51, C33, C51

«Ἤρξατο δὲ τὸ πρῶτον, ὡς λέγεται, ἐξ Αἰθιοπίας τῆς ὑπὲρ Αἰγύπτου, ἔπειτα δὲ καὶ ἐς Αἴγυπτον καὶ Λιβύην κατέβη καὶ ἐς τὴν βασιλέως γῆν /Περσία/ τὴν πολλήν.»

'It first began, it is said, in the parts of Ethiopia above Egypt, and thence descended into Egypt and Libya and into most of the King's country [i.e. Persia]'

Thucydides, 5th century B.C.

1. Introduction

The COVID-19 respiratory infection, caused by the SARS-CoV-2 virus first detected in Wuhan in late 2019, is continuing to spread globally with more than 530 million infections and 6.3 million deaths (7 June 2022; World Health Organization, WHO).[1] Due to the rapid spread of the virus, Dr Tedros Adhanom, WHO director-general, declared COVID-19 a pandemic on 11 March 2020. From the Great Plague of Athens (the first historically recorded epidemic in 430 B.C.) to the Black Death (the deadliest pandemic in the 14th century estimated to have killed 30–60% of Europe's population), humanity has faced several such fatal outbreaks. The most recent example of this magnitude is the 1918–9 influenza pandemic (the so-called 'Spanish flu').

Lessons from previous pandemics reveal that timeliness and stringency are crucial aspects for maximizing the effectiveness of non-pharmaceutical interventions (NPIs) and minimizing the adverse social and economic consequences (Hatchett et al., 2007; Martin et al., 2007; Dasgupta et al., 2021). Using historical data on the timing of 19 different types of NPIs in 17 US cities during the Spanish flu pandemic, Hatchett et al. (2007) show that implementation of multiple interventions at an early phase of the epidemic reduced peak death rates at a substantial magnitude (~50%). Statistical and epidemiological analyses of past data from several US cities also demonstrate that early, sustained, and layered application of public health measures contributed strongly to mitigating the consequences of the 1918-9 influenza pandemic in the USA (Martin et al., 2007).

This article quantifies the impact of NPIs, economic support measures (ESM), and their interplay, on the COVID-19 infections growth. We focus on the USA which has been severely hit by the COVID-19 pandemic. With more than 83.9 million coronavirus cases and 998,997 deaths on 7 June 2022,[1] the USA has the highest number of confirmed infections and the highest official death toll in the world (WHO). The first cases of COVID-19 occurred in January 2020 in travellers from China. Early travel restrictions imposed on 2 February 2020 to non-US citizens from China (later expanding to other countries with widespread transmission) failed to contain the virus, as the number of COVID-19 cases increased more than 1,000-fold during a 3-week period in late February to early March 2020 (Schuchat, 2020). The early epicentre was New York and the North-eastern states (New Jersey, Connecticut, and Massachusetts), where cases spiked in late March 2020. Social distancing restrictions brought infections down; however, their gradual relaxation led to new outbreaks, shifting to the South and West regions of the country (i.e. Arizona, Florida, and California) and leading to a new countrywide peak in July 2020.

In the absence of a centralized federal response, there has been extreme variability in the timing and intensity of interventions in the US states, and even at a county and city level (Adolph et al., 2021). Measures started being implemented only after 10 March 2020, 13 days after the first report of community transmission. California was the first state to enact a lockdown, followed by the Midwest and parts of the Northeast, as well as Louisiana. Later adopters were largely concentrated in the Middle Atlantic and upper Midwest. By 20 April 2020, 40 out of the 50 states had adopted state-wide lockdowns. Dave et al. (2021) estimate a decline of up to 43.7% in COVID-19 cases 3 weeks after the implementation of state-wide quarantine, with significant heterogeneity attributed to the timing of the enactment and state-specific characteristics. The social distancing effect of lockdown is estimated

1 See: https://covid19.who.int/; accessed: 7-6-2022.

to be twice as large for early as compared to later-adopting states (2.6% versus 1.3%). Dave et al. (2021) find that state-wide lockdowns are far more effective at decreasing the growth rate of coronavirus cases (including declines in the rate of COVID-19-related mortality) among early adopting states and states with higher population densities.

Chernozhukov et al. (2021) use data on confirmed COVID-19 cases and deaths for the US states to estimate panel data models. They find that nationally mandating face masks for employees early in the pandemic could have reduced the weekly growth rate of cases and deaths by more than 10 percentage points in late April 2020. Moreover, early enforcement of face masks could have led to as much as 19-47% less deaths nationally by the end of May 2020, which roughly translates into 19,000-47,000 saved lives. Their findings also suggest that in the absence of stay-at-home orders, cases would have been larger by 6-63% and without business closures, by 17-78%.

Drastic anti-contagion policy actions, such as national lockdowns, though effective, lead to unprecedented negative economic impact. The US economy experienced its deepest decline since official record keeping in 1947; indeed US Gross Domestic Product (GDP) shrank by an annualized rate of 32.9% in the second quarter of 2020 (https://fred.stlouisfed.org/; last accessed: 10 March 2021). Using high-frequency proxy measures of economic activity (e.g. NO_X emissions) for Europe and Central Asia, Demirgüç-Kunt et al. (2020) find that national lockdowns are associated with a decline in economic activity of around 10%. This economic cost puts governments under enormous pressure to relax the intensity of NPIs. Consequently, understanding the exact pairwise relationship between NPIs and the spread of COVID-19 (considering issues such as threshold effects and model misspecification) is important for governments to timely plan effective short-run interventions to tame infections and, at the same time, minimize the adverse impact on economic activity.

However, the current fast-growing literature assesses the effect of NPIs by hypothesizing a homogeneous impact, irrespective of their strength (e.g. Haug et al., 2020; Hsiang et al., 2020). We extend previous literature in two directions. First, we consider the impact of NPIs on infections depending on whether the stringency is too low, medium, or too strong. Secondly, we assess the role of the deployed ESM on COVID-19 infections; an issue that has largely been overlooked. In particular, we reveal the heterogeneous relationship between NPIs and the growth of COVID-19 confirmed cases, conditioning on a set of variables such as ESM and climatic conditions. To do so, we use US state-level data, and transform all variables through *backward-* or *forward-looking* rolling averages, thus accounting, to a certain extent, for errors in data measurement and most importantly for the endogenous nature of NPIs and COVID-19 infections. Moreover, as omitted variable bias may lead to invalid inferences, we estimate an augmented specification by including the ESM and the prevailing climatic conditions (temperature and relative humidity).[2] Indeed, in the presence of ESM, government interventions are likely to become more effective in bringing infection cases down. This is because employees, and the public in general, are more likely than not to stick to government intervention measures when economic support is in place. In addition, the spread of COVID-19 occurs predominantly via respiratory droplets and aerosols. In this case, temperature and relative humidity can affect transmission through virus survival. At lower temperatures, the virus survives longer and, at

2 As ESM are positively correlated with conducted government interventions, non-inclusion of these measures in the specification will lead to biased and inconsistent estimates.

lower humidity, infectious respiratory droplets and aerosols stay suspended in the air for longer.[3]

By fitting a two-threshold panel fixed-effect specification, we reach a number of findings. First, the impact of government NPIs on infections growth is significant and varies on the level of severity. We identify three distinct regimes, that is, regimes of 'low', 'medium', and 'high' severity interventions. A 10% increase in the level of the average NPIs (averaged over the previous 14 days) lowers the daily growth rate of infections by 0.35% in the 'low' regime, by 0.49% in the 'medium' regime, and by 0.55% in the 'high' regime. Secondly, ESM significantly bring COVID-19 cases growth down through a behavioural channel that lowers the workplace hours supplied by individuals. Thirdly, the efficacy of ESM towards suppressing COVID-19 cases growth depends on the severity of the deployed NPIs. Fourthly, climatic conditions affect the growth of COVID-19 cases; in particular, higher temperature and higher relative humidity reduce COVID-19 cases. Finally, the largest impact towards reducing infections comes jointly from school closures, workplace closures, cancelation of public events, and restrictions on internal movement, followed by the stay-at-home requirements, and the closure of public transport.

All in all, the main results of our article suggest that the stronger the NPIs the stronger the reduction in the growth rate of infections. This is arguably a desirable strategy not least because such action will restrict the chances of the virus mutating and transmitting even further. That said, the rolling out of vaccination programmes across the world should reduce the need or urgency for new lockdowns. It looks more likely than not that some NPIs will remain, for some time, in place not least because the ability of vaccination programmes to tackle the pandemic will depend on the implementation speed and their effectiveness in dealing with evolving virus mutations.

The article proceeds as follows: Section 2 discusses the data and model specification, Section 3 discusses the model estimates, and Section 4 presents the counterfactual analysis. Finally, Section 5 concludes.

2. Data and model specification

Being recently available by the Blavatnik School of Government of the University of Oxford, we use data on NPIs and ESM across all US states for the period spanning from 1 January to 4 August 2020 (Hale et al., 2021). We focus on the 50 US states using daily observations on (i) the strength of the NPIs policies at state level, proxied by the Oxford Covid-19 Government Response Tracker (OxCGRT) index,[4] (ii) the strength of the ESM,[4] (iii) the number of confirmed COVID-19 cases[5] and the state population estimates as of July 2019,[6] to construct the number of daily cases per 100,000, (iv) the temperature,[7] and (v) the relative humidity.[7]

3 See, for instance, the discussion in Ward et al. (2020). Wu et al. (2020) find that higher temperature and higher relative humidity result in lower COVID-19 cases and deaths using daily data for 166 countries.

4 Blavatnik School of Government, Oxford University (https://www.bsg.ox.ac.uk/; last accessed: 15-8-2020).

5 Centers for Disease Control and Prevention (https://www.cdc.gov/; last accessed: 15-8-2020).

6 United States Census Bureau, see: https://www.census.gov/; last accessed: 15-8-2020).

7 For temperature and relative humidity data, see NASA Langley Research Center, POWER Project, https://power.larc.nasa.gov/data-access-viewer/; last accessed: 20-8-2020).

The OxCGRT variable is a simple additive unweighted index that aggregates nine normalized individual containment and closure policies (school closures, workplace closures, cancelation of public events, restrictions on gathering size, closure of public transport, stay-at-home requirements, restrictions on internal movement, restrictions on international travel, and public information campaign). Each policy measure is quantified by a simple ordinal numerical scale (i.e. 0, 1, 2, and 3), reflecting its severity. Moreover, eight of these measures incorporate an additional dichotomous flag variable associated with geographical coverage (i.e. targeted region or state wide). For each policy measure, considering the maximum ordinal value and the respective maximum flag value (if applicable), the observed policy score is normalized to a scale ranging between 0 and 100. Thus, the overall OxCGRT index ranges between the same limits.

Similar in spirit is the construction of the ESM index. The ESM index aggregates two normalized individual economic support policies: income support (salary coverage or provision of direct cash payments, universal basic income to those who lose their jobs or are unable to work) and debt/contract relief for households (facilitation in meeting financial obligations, such as loan repayment and payment of basic utility bills). The income support sub-index also incorporates a binary flag variable associated with the sectoral coverage of the policy (i.e. excluding or including informal workers). Once the recorded values are available, the normalization of the two sub-indices and the construction of the ESM index follow the same process as the OxCGRT index.

To deal with endogeneity and measurement error (Raftery et al., 2020), variables are transformed through *forward-* or *backward-looking* rolling averages using a fixed window length.[8] We define the *forward-looking* transformation of a variable, at each time t, as the average value calculated by a fixed length rolling window with size equal to the 14 succeeding days.[9] Similarly, we define the *backward-looking* transformation by using the preceding 14 days. We first calculate the COVID-19 infections per 100,000 people and we then define, for each time t of the total sample, the *forward-looking* confirmed infections per 100,000 as the average of the succeeding 14 days. Based on the above transformation, we estimate the respective growth rate as the logarithmic difference of two subsequent observations. The *forward-looking* growth rate of infections per 100,000 (*growth of infections*, hereafter) for selected dates of the sample at state level is illustrated as a heat map in Supplementary Appendix Fig. A1.1. Supplementarily, the mean values of the variable aggregated at region/division level for the same sample dates are shown in Supplementary Appendix Table A1.1. Likewise, we define for each time t of the sample, the *backward-looking* OxCGRT index (*OxCGRT*, hereafter) and the *backward-looking* ESM index (*ESM*, hereafter) as the respective average of the preceding 14 days. The *OxCGRT* index for selected dates of the sample at state level is illustrated as column bars in Supplementary Fig. A1.1. Similarly, the mean values aggregated at region/division level are presented in Supplementary Appendix Table A1.1.

The *ESM* for selected dates of the sample, at state level, is illustrated as column bars in Supplementary Fig. A1.2, while the respective mean values at region/division level are reported in Supplementary Appendix Table A1.1. Supplementary Figure A1.2 and

8 Dasgupta et al. (2021) note that under-reporting infectious disease statistics is a common characteristic of the current pandemic and the 1665 London plague 350 years ago.

9 The window size is set to 14 days. Lauer et al. (2020) estimate that the virus incubation period is 14 days.

Supplementary Appendix Table A1.1 reveal that the bulk of the states acted decisively within a short period of time by deploying support measures to aid economic recovery. Although state responses were rapid, these appear to fluctuate considerably depending on the region/division. Well before the enforcement of federal stimulus through the Coronavirus Aid, Relief, and Economic Security (CARES) Act (27 March 2020), the state of Washington (Pacific division) was the first to put in place ESM in early January 2020. The state adjusted an existing unemployment insurance programme to aid employees who had their work hours reduced due to COVID-19 by covering up to 50% of their paycheck. On 21 March 2020, just before the enactment of the CARES Act, most of the states had in place some form of government subsidy in response to the pandemic. For the same date, the seven states illustrating an *ESM* score above 50 are New York, New Hampshire, Rhode Island, Alaska, Louisiana, Colorado, and New Jersey, with the vast majority being part of the Northeast and West (Pacific division) regions. In contrast, 16 states, mainly part of the South region (South Atlantic and East South Central divisions) and West region (Mountain division) had no ESM in place.

On 30 April 2020, a month after the enactment of the CARES Act, the *ESM* scores across all states increase considerably and become more homogeneous. The observed within-states variation is attributed to each state's individual choices on how to implement the federal stimulus. The overall emerging signal is that the states with the highest *ESM* scores are located in the Middle Atlantic and Pacific divisions. On 21 July 2020, the ESM remain at similar levels, following the same geographical distribution as on 30 April 2020. Overall, *ESM* in the early period of the pandemic (before CARES Act) vary widely among states as they rely heavily on state-specific policies. The federal stimulus in the later stage results to a more homogeneous state response, attributed to the mixture of state policies on top of the federal support.

We finally define, for each time, $\boldsymbol{t}$, of the total sample, the *backward-looking* temperature, as well as the *backward-looking* relative humidity. The *backward-looking* temperature variable for selected dates of the sample at state level is illustrated as column bars in Supplementary Appendix Fig. A1.3. The *backward-looking* relative humidity variable for selected dates at state level is illustrated as column bars in Supplementary Appendix Fig. A1.4.[10]

For all constructed *forward-* and *backward-looking* variables, we define the *effective sample* for each US state as the period signified by the first day with cumulative confirmed COVID-19 cases equal or greater than five, up to the end of the sample. Such treatment leads to a different *effective sample* in terms of time length for each US state (the maximum sample length with 170 observations corresponds to California, while the minimum sample length with 126 observations corresponds to Alaska, Hawaii, North Dakota, and West Virginia). As the fixed-effect panel threshold model necessitates a balanced sample, we use, from the effective sample of each US state, the first 126 observations. Hence, our final *feasible sample* (balanced sample) includes 126 observations for each US state.

Current literature (in the context of susceptible-infected-recovered [SIR] epidemiological models) assesses the effect of NPIs on COVID-19 infections (or deaths) assuming a homogeneous impact of these interventions irrespective of their strength (see Hsiang et al., 2020; Haug et al., 2020; Flaxman et al., 2020; Brauner et al., 2021). Under this strong

10 The mean values of both variables at region/division level are shown in Table A1.1 (see Supplementary Appendix 1).

assumption, any attempt to evaluate the exact effect of NPIs at their different levels is arguably misspecified. To overcome this limitation, we estimate for the 50 US states a panel fixed-effect threshold specification (Hansen, 1999), which remains robust to time-invariant differences (for the sample of our analysis) among the states (e.g. population density or income differences) and reveals the heterogeneous nature of the relationship between the *growth of infections* and NPIs. Moreover, as *ESM* are positively correlated with conducted government interventions, non-inclusion of these measures in the specification will lead to biased and inconsistent estimates. To reduce the impact of specification bias, the employed model is augmented with the inclusion of the *ESM* index and two climate variables (temperature and relative humidity). The model takes the form:

$$r_{it} = \delta + \vartheta_1 p_{it} I(p_{it} < k_1) + \vartheta_2 p_{it} I(k_1 \leq p_{it} < k_2) + \vartheta_3 p_{it} I(k_2 \leq p_{it}) + \varphi z_{it} + u_i + e_{it} \quad (1)$$

where, r_{it} is the *forward-looking* growth rate of infections per 100,000, δ and ϑ_j are parameters to be estimated (j =1,2,3), k_m are the threshold parameters (m =1, 2), p_{it} is the natural logarithm of the *backward-looking* OxCGRT index (threshold variable), I(·) is an indicator function which receives the value one if the condition in the parenthesis is true and zero otherwise, $\mathbf{z}_{it}$ is the matrix of the threshold-independent variables (the natural logarithm of the *backward-looking* ESM and the two *backward-looking* climate variables), φ is a vector of coefficients, u_i is the state individual effect, and e_{it} is the error term.

3. Threshold testing and estimation

To identify the number of significant thresholds for the *OxCGRT* index based on our benchmark econometric specification, Equation (1), we implement the sequential testing approach proposed by Hansen (1999). Thus, for testing sequentially the null hypotheses of zero, one, and two thresholds, we calculate the respective likelihood ratio F_j statistics (j =1,2,3), which follow a non-standard asymptotic distribution. To perform an inferential decision, within a bootstrap framework, we calculate p-values based on the empirical sampling distribution, which prove to remain valid asymptotically (Hansen, 1999). The three $F_j (j = 1, 2, \text{and } 3)$ statistics, along with the associated critical values at the conventional levels of significance and the bootstrapped p-values (with 1,000 replications), are analytically reported in Table 1.

Table 1 implies that the null hypothesis of zero thresholds against one threshold ($p = 0.002$) is rejected. We proceed by examining the null hypothesis of one threshold against two. The respective inference ($p = 0.002$) rejects the second null hypothesis, thus

Table 1. Testing for threshold effects

Threshold	Threshold estimate	Threshold at level	*F*-stat	*p*-Value	10% critical	5% critical	1% critical
Single	4.292***	73.149***	73.97	0.002	37.174	43.019	60.213
Double	3.375***	29.230***	59.25	0.003	29.485	34.552	48.841
Triple	3.753	42.657	41.15	0.283	55.603	65.412	91.846

Notes: *** denotes the rejection of the null hypothesis at the 0.01 significance level. All trimming values are set equal to 0.05. The reported critical values along with the respective *p*-values are derived by the bootstrap method with 1,000 replications. As the threshold variable is transformed in logarithmic form, each threshold estimate is converted to the level scale. *Source*: Authors' calculations.

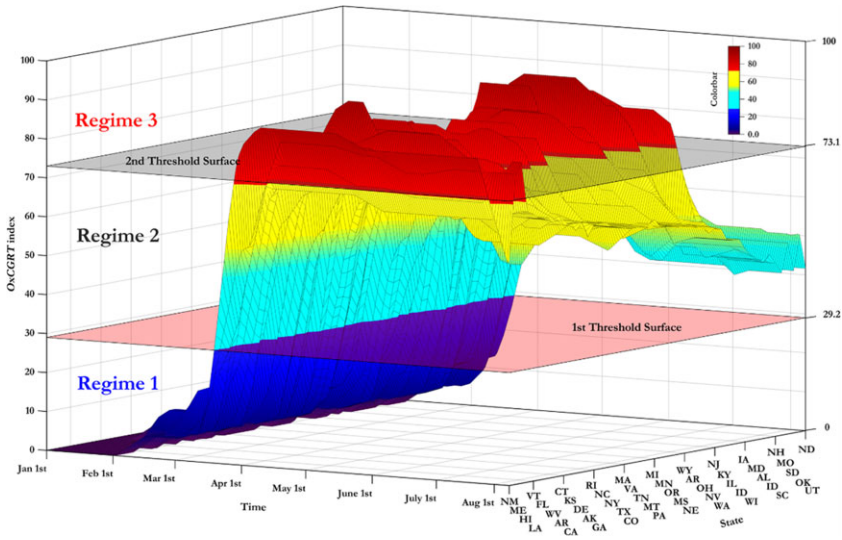

Fig. 1. OxCGRT index and estimated regimes. *Notes*: (i) The vertical left-axis depicts the stringency of the OxCGRT index; the bottom horizontal left-axis displays the date, and the bottom horizontal right-axis depicts the state (identified by the two-digit code abbreviation). (ii) The two-digit state abbreviations are: Alabama: AL, Alaska: AK, Arizona: AZ, Arkansas: AR, California: CA, Colorado: CO, Connecticut: CT, Delaware: DE, Florida: FL, Georgia: GA, Hawaii: HI, Idaho: ID, Illinois: IL, Indiana: IN, Iowa: IA, Kansas: KS, Kentucky: KY, Louisiana: LA, Maine: ME, Maryland: MD, Massachusetts: MA, Michigan: MI, Minnesota: MN, Mississippi: MS, Missouri: MO, Montana: MT, Nebraska: NE, Nevada: NV, New Hampshire: NH, New Jersey: NJ, New Mexico: NM, New York: NY, North Carolina: NC, North Dakota: ND, Ohio: OH, Oklahoma: OK, Oregon: OR, Pennsylvania: PA, Rhode Island: RI, South Carolina: SC, South Dakota: SD, Tennessee: TN, Texas: TX, Utah: UT, Vermont: VT, Virginia: VA, Washington: WA, West Virginia: WV, Wisconsin: WI, Wyoming: WY. (iii) The first and second thresholds of the OxCGRT index are signified by the pink and grey surface, respectively. (iv) The surface for the OxCGRT index is coloured based on the range of values assigned to each regime.

providing support for the presence of two thresholds. Finally, to discriminate between the presence of two or three thresholds, we test the third null hypothesis of two thresholds against three. The resulting evidence ($p = 0.283$) fails to reject the null hypothesis, signalling the existence of two significant thresholds. The point estimates for the two significant thresholds of the *OxCGRT* index are shown in Table 1. The first threshold estimate is 73.1 units (4.292 for the logarithmic transformation) and the second threshold estimate is 29.2 units (3.375 for the logarithmic transformation). The three resulting regimes range between [0-29.2], [29.2-73.1], and [73.1-100]. For our sample, Fig. 1 shows the two estimated thresholds (the two thresholds are signified by the pink and grey surface, respectively) along with the actual OxCGRT index in a three-dimensional coordinate system.

Figure 2 shows how the average *growth of infections* per US state is distributed across each regime. It becomes clear that the average *growth of infections* decreases as the regime level increases, confirming the validity of the estimated thresholds. Moreover, Table 2 presents the average values of each policy-specific indicator of the *OxCGRT* index in each regime. Table 2 reveals two interesting aspects. First, all specific policies contribute to all regimes but with different severity, and second, as we move from the lowest to the highest regime, with no exception, all specific policies show increasing severity.

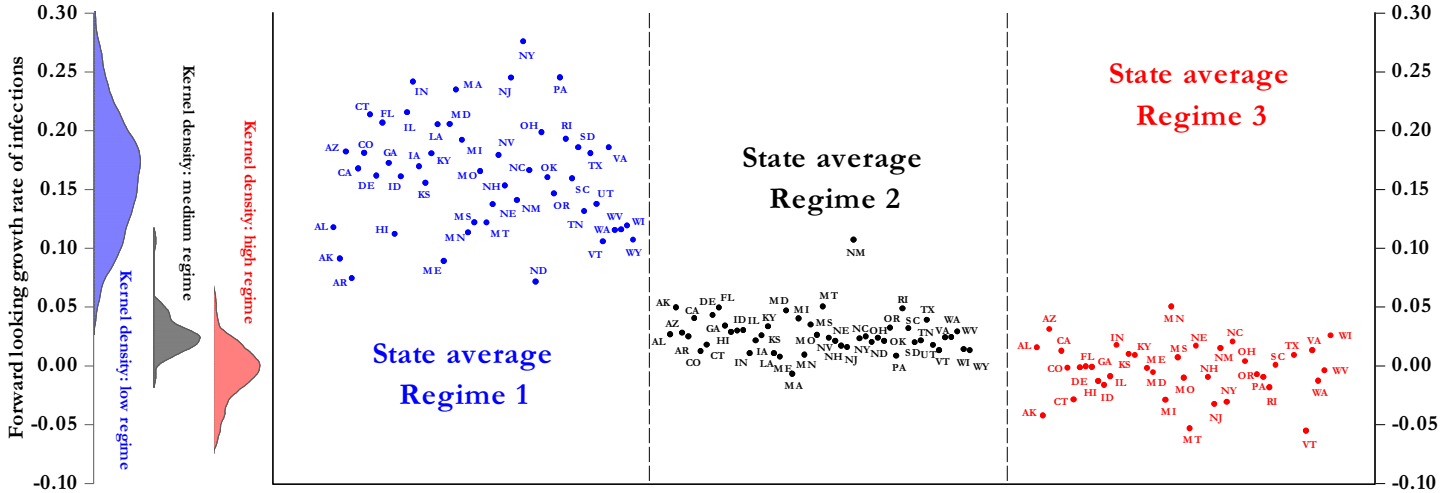

Fig. 2. Regime-dependent average *growth of infections* as per US states. *Notes*: (i) Regime 1, Regime 2, and Regime 3 are defined by the values of the threshold variable (the *backward-looking* OxCGRT index) that belong to (0–29.2), (29.2–73.1), and (73.1–100), respectively. (ii) Regime 1 and Regime 2 include all 50 US states, while Regime 3 includes 39 US states. The states that never have entered into Regime 3 are the following: Arkansas, Iowa, Louisiana, Massachusetts, Nevada, North Dakota, Oklahoma, South Dakota, Tennessee, Utah, and Wyoming. (iii) The kernel densities for the forward-looking growth rate of infections belonging in each regime, are presented at the left axis. Kernel density is a non-parametric approach for estimating the probability density function of a variable. (iv) The two-digit state abbreviations are: Alabama: AL, Alaska: AK, Arizona: AZ, Arkansas: AR, California: CA, Colorado: CO, Connecticut: CT, Delaware: DE, Florida: FL, Georgia: GA, Hawaii: HI, Idaho: ID, Illinois: IL, Indiana: IN, Iowa: IA, Kansas: KS, Kentucky: KY, Louisiana: LA, Maine: ME, Maryland: MD, Massachusetts: MA, Michigan: MI, Minnesota: MN, Mississippi: MS, Missouri: MO, Montana: MT, Nebraska: NE, Nevada: NV, New Hampshire: NH, New Jersey: NJ, New Mexico: NM, New York: NY, North Carolina: NC, North Dakota: ND, Ohio: OH, Oklahoma: OK, Oregon: OR, Pennsylvania: PA, Rhode Island: RI, South Carolina: SC, South Dakota: SD, Tennessee: TN, Texas: TX, Utah: UT, Vermont: VT, Virginia: VA, Washington: WA, West Virginia: WV, Wisconsin: WI, Wyoming: WY.

Table 2. Average values of the policy-specific *OxCGRT* indices across states and within each regime

OxCGRT policy specific indices	Regime 1	Regime 2	Regime 3
1. School closures	7.51	74.98	89.62
2. Workplace closures	7.71	56.78	85.38
3. Cancelation of public events	10.06	73.12	97.12
4. Restrictions on gathering size	4.68	64.62	95.82
5. Closure of public transport	0.70	13.73	32.23
6. Stay-at-home requirements	1.18	32.89	58.97
7. Restrictions on internal movement	4.08	54.00	80.39
8. Restrictions on international travel	68.92	75.00	75.00
9. Public information campaign	51.54	98.43	99.42

Notes: The average values of each sub-index refer to the transformed index through *backward-looking* rolling averages using a fixed length 14-day window. *Source*: Authors' calculations.

For the balanced *feasible sample*, we fit a fixed-effect panel specification with two thresholds by implementing the typical fixed-effect estimator, Equation (1). These estimates, along with the associated standard errors, clustered at the state level, are presented in the first column of Table 3. The second column illustrates the same estimates but with block bootstrapped standard errors at the state level. Before executing any statistical inference, we conduct some diagnostic testing for the first column estimates.

Thus, we test for: (i) the strict exogeneity of the *OxCGRT* and *ESM* indices; (ii) groupwise homoscedasticity; (iii) serial correlation; and (iv) cross-sectional independence. The test for strict exogeneity proposed by Wooldridge (2010), supports that both the *OxCGRT* ($p = 0.295$) and *ESM* ($p = 0.324$) indices are strictly exogenous.[11] Moreover, we test for groupwise homoscedasticity by the modified Wald's statistic (see Greene, 2000). The respective evidence ($p = 0.000$) implies that the error term violates the assumption of homoskedasticity. On top of the above violation, the error term appears to be serially correlated as the Lagrange Multiplier (LM) statistic (Born and Breitung, 2016) rejects the null hypothesis of uncorrelated residuals of first order ($p = 0.000$). Finally, by implementing a parametric testing procedure for examining the cross-sectional independence of the residuals (Pesaran, 2021), we find that these are cross-sectionally dependent ($p = 0.045$) at the 0.05 significance level. Overall, the diagnostic testing reveals that the *OxCGRT* and *ESM* indices are strictly exogenous; nevertheless, it shows that the model suffers from heteroscedasticity, serial correlation, and cross-sectional dependence.

As the executed diagnostic testing reveals the existence of a non-spherical error term, the initial fixed-effect estimates are expected to be inefficient and their associated standard errors biased, rendering all resulting inferences questionable. Hence, we re-estimate our specification by implementing approaches that are robust to the above-mentioned forms of misspecification. We continue by reporting the Parks (1967) feasible generalized least squares estimates (FGLS) (Column 3), which deliver standard errors that remain robust to heteroscedasticity, as well as to general forms of cross-sectional and temporal dependence.

11 For a linear fixed-effect model without strictly exogenous regressors, Nerlove (1967) provides simulation evidence that the estimator is biased, while Nickell (1981) analytically characterizes the bias.

Table 3. Threshold panel fixed-effect estimation results

Variable	FEC (1)	FEBB (2)	FGLS (3)	PCSE (4)	PCSE (5)
Constant	0.3736***	0.3736***	0.3451***	0.3307	0.3313***
	(0.0853)	(0.0496)	(0.0148)	(0.0350)	(0.0347)
Humidity	−0.0008***	−0.0008***	−0.0004***	−0.0008***	−0.0008***
	(0.0003)	(0.0002)	(0.0001)	(0.0002)	(0.0002)
Temperature	−0.0008**	−0.0008***	−0.0003**	−0.0005**	−0.0005*
	(0.0004)	(0.0002)	(0.0001)	(0.0002)	(0.0002)
ESM	−0.0050	−0.0050**	−0.0060***	−0.0063***	–
	(0.0038)	(0.0019)	(0.0010)	(0.0023)	
Regime slopes					
$OxCGRT_{R1}$	−0.0492*	−0.0492***	−0.0536***	−0.0367***	−0.0373***
	(0.0263)	(0.0163)	(0.0038)	(0.0092)	(0.0092)
$OxCGRT_{R2}$	−0.0635***	−0.0635***	−0.0639***	−0.0516***	−0.0518***
	(0.0207)	(0.0126)	(0.0031)	(0.0075)	(0.0076)
$OxCGRT_{R3}$	−0.0684***	−0.0684***	−0.0673***	−0.0573***	−0.0442***
	(0.0200)	(0.0120)	(0.0030)	(0.0073)	(0.0141)
ESM_{R1}	–	–	–	–	−0.0054
					(0.0048)
ESM_{R2}	–	–	–	–	−0.0065***
					(0.0024)
ESM_{R3}	–	–	–	–	−0.0199
					(0.0128)
Summary statistics					
n	6300	6300	6300	6300	6300
R^2-within	0.35	0.35	–	0.26	0.26
F/Wald X^2	0.000	0.000	0.000	0.000	0.000
Diagnostic testing (column 1)					
Strict exogeneity test (*p*-value)			Homoskedasticity test (*p*-value)		0.000
	OxCGRT	0.295	Serial correlation test (*p*-value)		0.000
	ESM	0.324	CSD test (*p*-value)		0.045

Notes:***, **, and * denote statistical significance at the 0.01, 0.05, and 0.1 significance level, respectively. The reported values within the (.) are standard errors. The subscripts R1, R2, and R3 signify the three regimes. The columns titled as FEC, FEBB, FGLS, and PCSE refer to the threshold panel fixed-effect estimates (i) with standard errors clustered at the state level, (ii) with block bootstrapped standard errors at the state level, (iii) with the use of the feasible generalized least squares approach, and (iv) with the PCSE estimation approach, respectively. *Source*: Authors' calculations.

Moreover, provided that the FGLS estimator proves to perform poorly in finite samples, we report the Beck and Katz (1995) panel-corrected standard error (PCSE) estimation results (Column 4).

The PCSE estimation results (Column 4) reveal that all explanatory variables are significant at conventional levels of significance (mainly at the 0.01 level). Most importantly, the *OxCGRT* index, throughout its entire range, remains effective at decreasing the *growth of*

infections, albeit with a different impact at each regime. Additionally, *ESM* have a negative and statistically significant effect, a finding that also holds true for the two climatic variables. Given the presence of the thresholds, the model fits the data satisfactorily, as judged by Fig. 3(a and b), which show the raw actual values of the *growth of infections* per US state and the model's respective fitted values along with the 99% confidence interval.

Based on the PCSE estimation results (Column 4), we identify a negative and statistically significant impact of the *backward-looking* temperature ($p < 0.05$) and the *backward-looking* relative humidity ($p < 0.01$) on the *growth of infections*. An increase by one degree Celsius in the *backward-looking* temperature lowers, on average, the daily *growth of infections* by 0.05%, while the respective impact for a unit increase in the *backward-looking* relative humidity is 0.08%. Moreover, the *growth of infections* at all regimes is related negatively and in a statistically significant manner ($p < 0.01$) to the *OxCGRT* index. More specifically, the regime-dependent coefficients with the associated 95% confidence intervals are −0.037 [−0.055, −0.019], −0.052 [−0.066, −0.037], and −0.057 [−0.072, −0.043] for the 'low', 'medium', and 'high' regime, respectively. The coefficient for the 'low' regime ('medium' regime), ['high' regime] suggests that a 10% increase in the level of the *OxCGRT* index lowers the daily percentage *growth of infections*, on average, by 0.35%, (0.49%), [0.55%]. Overall, the *OxCGRT* index throughout its entire range remains effective at decreasing the *growth of infections*, albeit with a different impact at each regime. Moreover, we find a significant ($p < 0.01$) impact of the *ESM* on the *growth of infections*. The magnitude of the coefficient implies that a 10% increase in the *ESM* lowers the daily percentage *growth of infections*, on average, by 0.06%. *ESM* can be viewed as an important factor, since the population will more likely adhere to government intervention measures when combined with additional economic support.[12]

Not unexpectedly, even with the presence of fixed effect in the estimated specification, our hypothesis that ESM drive supplemental compliance to NPIs can be questioned. One could argue that in high-income states, where expanded ESM are on offer, people may be more likely to voluntarily follow NPIs if they have a greater fear of the virus or they place greater trust in science (and policy experts). For instance, Singh et al. (2021) show that in high-income states, where people are more likely to be able to work from home, compliance rates with NPIs are higher. Therefore, the underlying mechanism that leads to added compliance may be attributed to factors other than those suggested by our hypothesis. Thus, additional theoretical and empirical support is deemed necessary to validate this hypothesis.

A theoretical justification for this hypothesis can be traced to models that integrate the epidemiological block and the economic block to a unified framework; the so-called SIR

12 As an extension, we examine the impact of the disaggregated policy-specific interventions (for both *OxCGRT* and *ESM* indices) on the *growth of infections*. Thus, by turning to the raw data, we rebuild policy specific indices following the same methodology implemented for the two aggregate indices. Within the framework of a panel specification with fixed-effect, we find that the largest impact in lowering the *growth of infections* comes from workplace closures, followed by the restrictions on internal movement, the income support, the closure of public transport, and stay-at-home requirements. However, given the presence of collinear regressors, we re-estimate an additional specification by aggregating all the collinear indices to form new ones (reducing this way dimensionality). The new findings reveal that the largest impact in lowering the *growth of infections* comes from the joint index of school closures, workplace closures, cancelation of public events, and restrictions on internal movement, followed by the stay-at-home requirements and the closure of public transport. These results are presented in Supplementary Appendix 2.

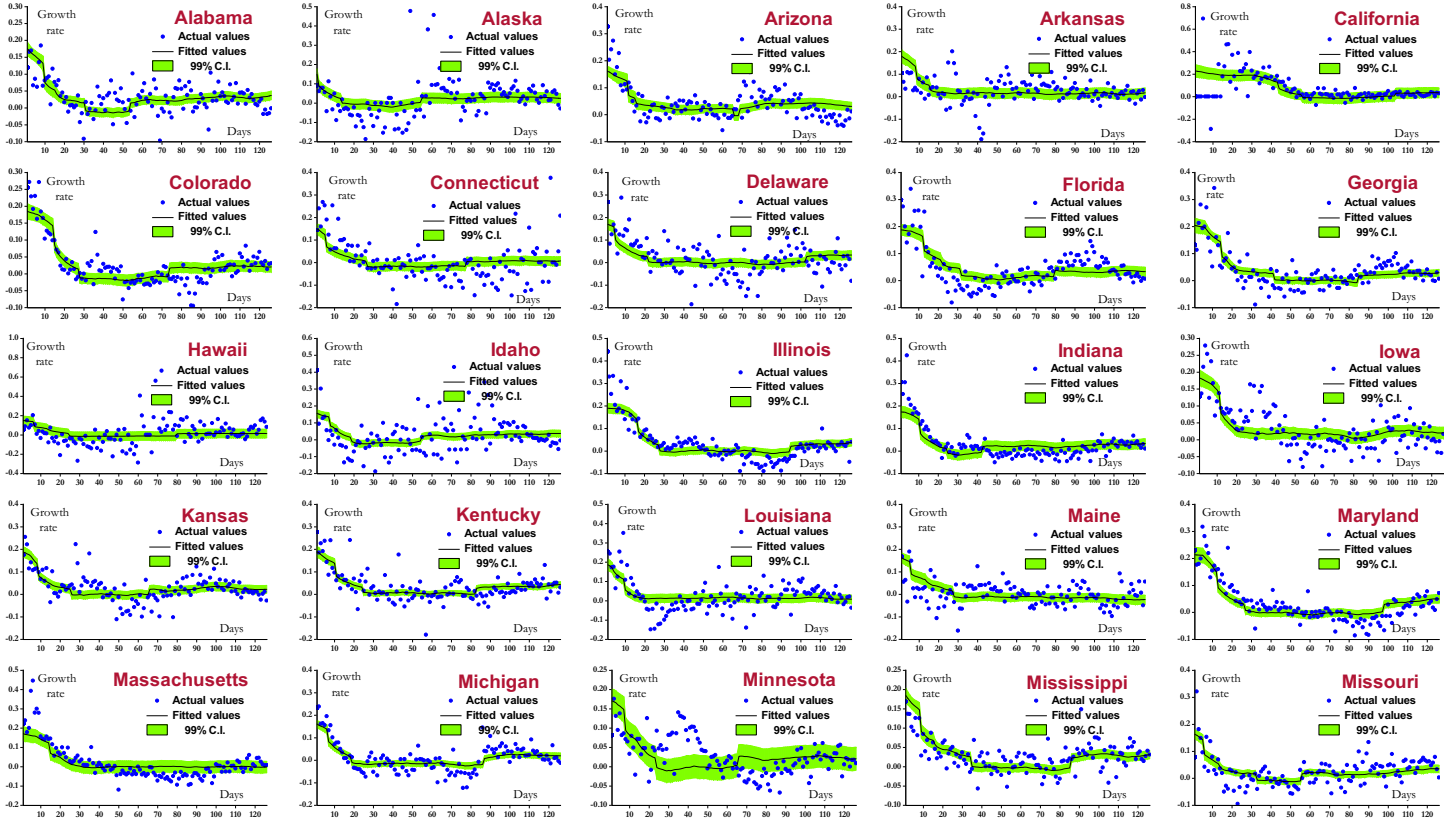

Fig. 3. (a) COVID-19 *growth of infections* per U.S. state: actual and fitted values along with respective 99% confidence interval. *Notes*: Estimates are based on the threshold panel fixed-effect model, Equation (1), using the (PCSE estimation approach (see Table 3, Column 4). (b) COVID-19 *growth of infections* per US state: actual and fitted values along with respective 99% confidence interval. *Notes*: Estimates are based on the threshold panel fixed-effect model, Equation (1), using the PCSE estimation approach (see Table 3, Column 4).

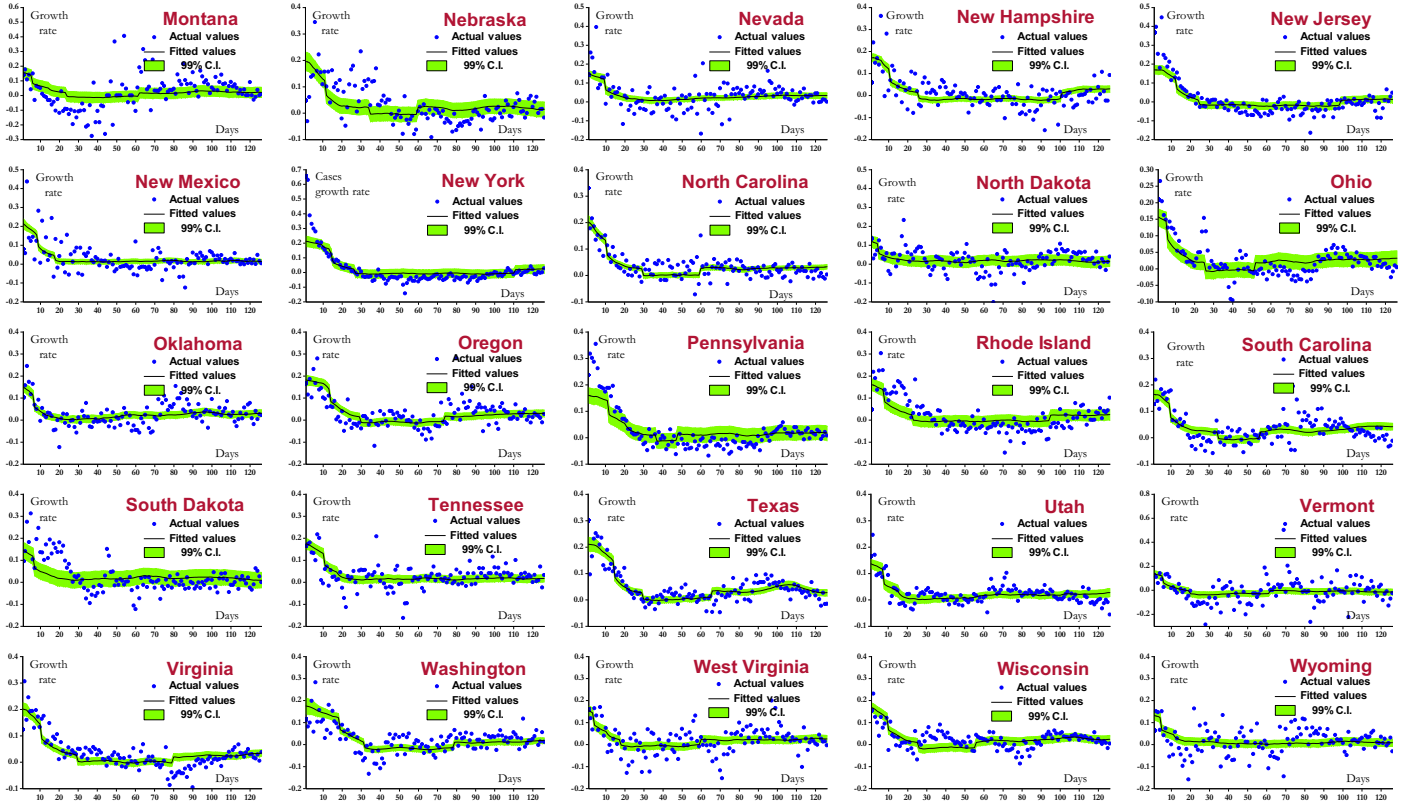

Fig. 3. Continued

-macro models (see among others, Ansah et al., 2020; Baqaee and Farhi, 2020; Kaplan et al., 2020). Specifically, Kaplan et al. (2020) model the impact of ESM on the pandemic by allowing governments to subsidize wage payments and profits. While these policies impact individuals' holdings of liquid wealth, their choices over the total supply of labour are adjusted. As long as ESM result in a positive income effect, individuals are willing to work fewer hours in the workplace. Provided that the virus transmission rate depends positively on the aggregate workplace hours (Equation (3), in Kaplan et al., 2020), lower workplace hours result in fewer infections. Consequently, through this behavioural mechanism, the ESM affect the virus transmission rate in parallel to NPIs.[13]

The above behavioural mechanism is also supported by some relevant studies. For instance, Andersen et al. (2021) rely on cellular device data and use difference-in-differences to assess the impact of the national paid sick leave policy implemented in the USA in April 2020. According to their findings, the policy reduced the average number of hours not at home by 8.9% and also reduced the share of the individuals likely at work (defined as away from their home for $\geq$8 h /day) by 6.9%. Bodas and Peleg (2020) assess public compliance rates in Israel depending on whether lost wages would be compensated for. According to their cross-sectional survey conducted in February 2020, the compliance rate to COVID-19-related lockdown rules was 94% under the assumption of lost wages being compensated, but dropped to <57% in the absence of compensation. Last, but not the least, an OECD (2020) report on policy responses to the COVID-19 virus reviews the ESM of OECD countries towards workers and their families to argue that economic support helps contain the spread of the virus and preserving jobs.

Moreover, given the three identified regimes for the *OxCGRT* index, we may further assess the validity of the behavioural mechanism. Intuitively, when containment policies are not very stringent (in the 'low' regime) or are too draconian (in the 'high' regime), ESM cannot be that effective towards suppressing infections. In particular, in the 'low' regime the economic support policies are not yet deployed to the extent that would drive the activation of this behavioural mechanism (in this 'low' regime, economic support is sporadically in force and at a very low severity; the average value of the *ESM* index across all states is just 2.47). On the other hand, in the 'high' regime, individuals do not have the choice of adjusting their work hours in the workplace, since policies such as 'workplace closing' and 'stay-at-home' requirements are in force (both interventions, in the 'high' regime, are continuously in force and at high severity; the average values of the two sub-indices across states are 85.38 and 58.97, respectively; see Table 2). Thus, we proceed by estimating one additional specification (see Column 5; Table 3) in which the *ESM* variable is incorporated within the three regimes identified through the *OxCGRT* variable. The empirical results in Column 5 of Table 3 support the main findings reported in Column 4 of Table 3. Nevertheless, they also show that *ESM* reduce in a statistically significant manner the *growth of infections*

13 To empirically evaluate the behavioural mechanism that stems from the theoretical context of Kaplan et al. (2020), we collect data for the change in workplace mobility (from the Community Mobility Reports database of Google). By implementing a typical panel fixed-effect specification, we regress the change in workplaces mobility on: (i) *OxCGRT*, (ii) *ESM*, (iii) the state of the pandemic, (iv) the individuals learning behaviour, and (v) two dummies capturing state-specific holidays and federal holidays. The results show that *ESM* significantly reduce workplace mobility supporting this way our hypothesis. These empirical results are analytically presented in Supplementary Appendix 3.

only in the 'medium' regime. In the remaining two regimes ('low' and 'high'), the *ESM* variable is statistically insignificant. Therefore, the impact of *ESM* becomes significant in reducing the *growth of infections* in the 'middle' regime, where individuals are permitted to adjust their work hours in the workplace and economic aid is in force. In other words, this finding can be seen as a validation of the behavioural mechanism that permits economic support policies to become effective in reducing the *growth of infections*.

Lastly, to evaluate the sensitivity of our estimates when *forward*- and *backward*-moving average transformations of different window sizes are implemented in the variables, we repeat the estimation of Equation (1) for a set of different window sizes (10, 7, and 5), as well as for the non-transformed variables (see Supplementary Appendix 4). Doing so, we find that the estimates for the regime-dependent variable are relatively unaffected by the window size (with regards to the number of the significant thresholds, the sign, the significance, and the impact), although this is not the case for the non-transformed variables. When no transformation is applied, the regime-dependent *OxCGRT* variable is insignificant and most importantly with incorrect signs across all regimes. Moreover, the transformation process and the window size both matter for attaining higher R^2 values and for establishing exogeneity. Therefore, these results validate the use of the *forward*- and *backward*-moving average transformation with the selected 14-day window size.

4. Counterfactual analysis

We use the PCSE estimates of Column 4 in Table 3 to run a series of counterfactual scenarios. We hypothesize different levels of the *OxCGRT* index that remain constant across the sample and derive their impact. We start by estimating, per US state, the *growth of infections* assuming no government action. We then estimate the respective *growth of infections* for sequential increase of the *OxCGRT* index by 10 units and up to 100, creating this way the response surface illustrated in Supplementary Appendix Fig. A5.1, which also shows the *growth of infections* across all states at the two estimated thresholds. Detailed counterfactual results are reported in Supplementary Appendix Table A5.1.

In the absence of government action, the average daily percentage *growth of infections* for all states is estimated at 24% (see the last row of Supplementary Appendix Table A5.1). The analysis suggests that the pursued government intervention policies reduced the average daily percentage *growth of infections* by 21.4 percentage points (Supplementary Appendix Table A5.1) compared to the case where no action had taken place. This difference is significant ($p < 0.01$). Considering the other extreme, that is, government intervention at the highest stringency level, the average daily percentage growth of infections is −2.3% (Supplementary Appendix Table A5.1). Had, therefore, government intervention remained at its highest stringency level throughout the sample, the average daily growth rate of infections would have been lower by 4.9 percentage points (Supplementary Appendix Table A5.1) compared to the impact of the actual government intervention policies. The difference is, again, significant ($p < 0.01$).

Since the increasing strength of NPIs harms economic activity, it is essential to identify the minimum level of measures capable of reverting the growth rate of infections to negative values. By setting the government interventions level equal to the second threshold, the average daily percentage *growth of infections* turns negative for the first time and equal to −0.60% (Supplementary Appendix Table A5.1). This estimate is lower by 3.2 percentage points ($p < 0.01$) compared to the impact of the actual policies. Overall, the counterfactual

analysis suggests that while NPIs are effective in reducing the *growth of infections* at all magnitudes, negative growth rates can be achieved only when government stringency is set to a level being part of the 'high' regime (73.1-100).

What happens if we switch attention to the individual US states? Had the level of government interventions remained at the second threshold, the state of California would have achieved the largest reduction in the *growth of infections* by a daily average of 6.2 percentage points ($p < 0.01$), followed by North Dakota (reduction of 5 percentage points; $p < 0.01$) and Oklahoma (reduction of 4.9 percentage points; $p < 0.01$; Supplementary Appendix Table A5.1). Our model implies that these US states would have achieved even larger reductions in the average daily *growth of infections* (8, 6.8, and 6.7 percentage points for California, North Dakota, and Oklahoma, respectively, and in all cases with a $p < 0.01$) had government intervention remained at its highest stringency level throughout the sample, compared to the actual implemented policies.

We proceed by running a set of counterfactual scenarios for the *ESM* index. We report in Supplementary Appendix Fig. A5.2, per US state, the *growth of infections* for a 10-unit sequential increase of the *ESM* index from 0 to 100. Detailed counterfactual results are reported in Supplementary Appendix Table A5.2. In the absence of economic support, the average daily percentage *growth of infections* is estimated at 5% (see the last row of Supplementary Appendix Table A5.2). At the opposite extreme, the respective percentage growth is estimated at 2.1% (Supplementary Appendix Table A5.2). When compared to the actual government economic interventions, both scenarios illustrate statistically significant differences ($p < 0.01$). Specifically, actual deployed *ESM* reduced the average daily percentage *growth of infections* by 2.4 percentage points compared to no *ESM*. In addition, had *ESM* been implemented at their highest level, the average daily percentage *growth of infections* would have been lower by 0.5 percentage points. Overall, government *ESM* act complementarily to NPIs in significantly reducing further the *growth of infections*. That said, an obvious limitation of the counterfactual analysis executed in this section is that we do not model individual behaviour. In other words, we assume no endogenous behaviour responses to the counterfactual levels of the *OxCGRT* and *ESM* indices. Consequently, one should interpret the counterfactual values calculated here as upper and lower bounds on the counterfactual *growth of infections*.

5. Conclusions

We examine, for the US states, the pairwise relationship between NPIs and the growth of COVID-19 confirmed cases by allowing government interventions to affect infections in a heterogeneous manner based on their varying strength. Using a two-threshold panel fixed-effect specification and conditioning on a set of regime-independent variables, such as *ESM* and climatic conditions, we reach a number of findings. First, we identify three distinct regimes of 'low', 'medium', and 'high' severity interventions; interventions have a stronger impact in reducing infections at the 'high' regime. Secondly, ESM reduce the growth of COVID-19 cases through a behavioural channel that lowers the workplace hours supplied by individuals. Thirdly, the efficacy of ESM towards suppressing COVID-19 cases growth depends on the severity of the deployed NPIs. Fourthly, climatic conditions affect the growth of COVID-19 cases. Last but not the least, the largest impact towards reducing infections growth is achieved jointly

from school closures, workplace closures, cancelation of public events, and restrictions on internal movement, followed by the stay-at-home requirements and the closure of public transport.

Our article contributes to the understanding of the exact pairwise regime-dependent relationship between containment measures and confirmed cases by quantifying in a heterogeneous manner the impact of government interventions on COVID-19 infections. Our findings seek to allow policymakers to timely plan more effective short-run interventions towards handling infections. In addition, our findings seek to inform policymakers on how to minimize the negative impact of government pandemic-related policies on economic activity and achieve cost savings in the health sector and efficient allocation of existing (but nonetheless limited) resources.

Based on the results of our article, it might be tempting to argue that stronger government interventions, in excess of the high threshold, might have to be put in place to reduce the growth rate of COVID-19 infections, not the least because such action will arguably restrict the chances of the virus evolving even further. That said, our results do not consider the rolling out of the vaccination programme which took effect from December 2020 onwards. The emergence of mutated COVID-19 variants with higher transmissibility (Kupferschmidt, 2021) seems to suggest that the success of the vaccination programme towards controlling the pandemic will depend, among other things, (i) on how fast the virus mutates, (ii) on whether new versions of the approved vaccines can be rolled out in a speedy manner to tackle the variants of the virus, and (iii) on vaccine acceptance.[14] All in all, it makes sense to expect that some NPIs measures will remain in place even as the vaccination programme 'attacks' the pandemic.

Supplementary material

Supplementary material is available online on the OUP website. These are the data and replication files and the online appendices.

Funding

This work was supported by the Hellenic Foundation for Research and Innovation (H.F.R.I.) under the 4th Call for Action 'Science and Society'- Emblematic Action- 'Interventions to address the economic and social effects of the COVID-19 pandemic' [4882 to T.D.].

Acknowledgements

We thank a reviewer of this journal for very useful comments and suggestions. We have also benefitted from comments of seminar participants at Trinity Business School, Trinity College Dublin.

14 In collaboration with Facebook, the Delphi group at Carnegie Mellon University conducts research surveys to monitor vaccine acceptance (percentage of people who either have already received a COVID vaccine or would definitely or probably choose to receive one if it were offered to them today) in the USA. In April 2022, vaccine acceptance stood at 84.17%. This was roughly the same as the vaccine acceptance of 84.43% almost a year earlier in May 2021.

See: https://delphi.cmu.edu/covidcast/survey-results/?date=20220401; last accessed: 10-5-2022).

References

Adolph, C., Amano, K., Bang-Jensen, B., Fullman, N., and Wilkerson, J. (2021) Pandemic politics: Timing State-Level social distancing responses to COVID-19, *Journal of Health Politics, Policy and Law*, **46**, 211–33.

Andersen, M., Maclean, J.C., Pesko, M.F., and Simon, K.I. (2021). Paid sick-leave and physical mobility: Evidence from the United States during a pandemic, National Bureau of Economic Research, NBER Working Paper, No. 27138, Cambridge, MA.

Ansah, J.P., Epstein, N., and Nalban, V. (2020) COVID-19 impact and mitigation policies: a didactic Epidemiological-Macroeconomic model approach, International Monetary Fund, IMF Working Papers, 20, Washington, DC.

Baqaee, D. and Farhi, E. (2020). Supply and demand in disaggregated Keynesian economies with an application to the covid-19 crisis, National Bureau of Economic Research, NBER Working Paper, No. 27152, Cambridge, MA.

Beck, N. and Katz, J.N. (1995) What to do (and not to do) with time series cross-section data, *American Political Science Review*, **89**, 634–47.

Bodas, M. and Peleg, K. (2020) Self-isolation compliance in the COVID-19 era influenced by compensation: findings from a recent survey in Israel, *Health Affairs (Project Hope)*, **39**, 936–41.

Born, B. and Breitung, J. (2016) Testing for serial correlation in fixed-effects panel data models, *Econometric Reviews*, **35**, 1290–316.

Brauner, J.M., Mindermann, S., Sharma, M., Johnston, D., Salvatier, J., Gavenčiak, T., Stephenson, A.B., Leech, G., Altman, G., Mikulik, V., Norman, A.J., Monrad, J.T., Besiroglu, T., Ge, H., Hartwick, M.A., Whye, Y., Chindelevitch, L., Gal, Y., and Kulveit, J. (2021) Inferring the effectiveness of government interventions against COVID-19, *Science*, **371**, eabd9338.

Chernozhukov, V., Kasahara, H., and Schrimpf, P. (2021) Causal impact of masks, policies, behavior on early covid-19 pandemic in the US, *Journal of Econometrics*, **220**, 23–62.

Dasgupta, U., Jha, C.K., and Sarangi, S. (2021) Persistent patterns of behavior: Two infectious disease outbreaks 350 years Apart, *Economic Inquiry*, **59**, 848–57.

Dave, D., Friedson, A.I., Matsuzawa, K., and Sabia, J.J. (2021) When do shelter-in-Place orders fight COVID-19 best? Policy heterogeneity across states and adoption time, *Economic Inquiry*, **59**, 29–52.

Demirgüç-Kunt, A., Lokshin, M., and Torre, I. (2020). The sooner, the better: The early economic impact of non-pharmaceutical interventions during the COVID-19 pandemic, The World Bank, Policy Research Working Paper Series 9257, Washington, DC.

Flaxman, S., Mishra, S., Gandy, A., Unwin, H.J.T., Mellan, T.A., Coupland, H., Whittaker, C., Zhu, H., Berah, T., Eaton, J.W., Monod, M., Perez-Guzman, P.N., Schmit, N., Cilloni, L., Ainslie, K.E.C., Baguelin, M., Boonyasiri, A., Boyd, O., Cattarino, L., Cooper, L.V., CucunubÄ, Z., Cuomo-Dannenburg, G., Dighe, A., Djaafara, B., Dorigatti, I., van Elsland, S.L., FitzJohn, R.G., Gaythorpe, K.A.M., Geidelberg, L., Grassly, N.C., Green, W.D., Hallett, T., Hamlet, A., Hinsley, W., Jeffrey, B., Knock, E., Laydon, D.J., Nedjati-Gilani, G., Nouvellet, P., Parag, K.V., Siveroni, I., Thompson, H.A., Verity, R., Volz, E., Walters, C.E., Wang, H., Wang, Y., Watson, O.J., Winskill, P., Xi, X., Walker, P.G.T., Ghani, A.C., Donnelly, C.A., Riley, S., Vollmer, M.A.C., Ferguson, N.M., Okell, L.C., and Bhatt, S., Imperial College COVID-19 Response Team. (2020) Estimating the effects of non-pharmaceutical interventions on COVID-19 in Europe, *Nature*, **584**, 257–61.

Greene, W. (2000). *Econometric Analysis*, Prentice-Hall, Upper Saddle River, NJ.

Hale, T., Angrist, N., Goldszmidt, R., Kira, B., Petherick, A., Phillips, T., Webster, S., Cameron-Blake, E., Hallas, L., Majumdar, S., and Tatlow, H. (2021) A global panel database of pandemic policies (oxford COVID-19 government response tracker), *Nature Human Behaviour*, **5**, 529–38.

Hansen, B.E. (1999) Threshold effects in non-dynamic panels: Estimation, testing, and inference, *Journal of Econometrics*, **93**, 345–68.

Hatchett, R.J., Mecher, C.E., and Lipsitch, M. (2007) Public health interventions and epidemic intensity during the 1918 influenza pandemic, *Proceedings of the National Academy of Sciences of the United States of America*, **104**, 7582–7.

Haug, N., Geyrhofer, L., Londei, A., Dervic, E., Desvars-Larrive, A., Loreto, V., Pinior, B., Thurner, S., and Klimek, P. (2020) Ranking the effectiveness of worldwide COVID-19 government interventions, *Nature Human Behaviour*, **4**, 1303–12.

Hsiang, S., Allen, D., Annan-Phan, S., Bell, K., Bolliger, I., Chong, T., Druckenmiller, H., Huang, L.Y., Hultgren, A., Krasovich, E., Lau, P., Lee, J., Rolf, E., Tseng, J., and Wu, T. (2020) The effect of large-scale anti-contagion policies on the COVID-19 pandemic, *Nature*, **584**, 262–7.

Kaplan, G., Moll, B., and Violante, G.L. (2020). The great lockdown and the big stimulus: Tracing the pandemic possibility frontier for the US, National Bureau of Economic Research, NBER Working Paper, No. 27794, Cambridge, MA.

Kupferschmidt, K. (2021) Viral evolution may herald new pandemic phase, *Science (New York, N. Y.)*, **371**, 108–9.

Lauer, S., Grantz, K.H., Bi, Q., Jones, F.K., Zheng, Q., Meredith, H.R., Azman, A.S., Reich, N.G., and Lessler, J. (2020) The incubation period of coronavirus disease 2019 (COVID-19) from publicly reported confirmed cases: Estimation and application, *Annals of Internal Medicine*, **172**, 577–82.

Martin, C., Bootsma J., and Ferguson, N.M. (2007). The effect of public health measures on the 1918 influenza pandemic in US cities, *Proceedings of the National Academy of Sciences United States of America*, **104**, 7588–93.

Nerlove, M. (1967) Experimental evidence on the estimation of dynamic economic relations from a time series of cross-section, *The Economic Studies Quarterly*, **18**, 42–74.

Nickell, S. (1981) Biases in dynamic models with fixed effects, *Econometrica*, **49**, 1417–26.

OECD. (2020). *Paid Sick Leave to Protect Income, Health and Jobs through the COVID-19 Crisis. OECD Policy Responses to Coronavirus (COVID-19)*, OECD Publishing, Paris.

Parks, R. (1967) Efficient estimation of a system of regression equations when disturbances are both serially and contemporaneously correlated, *Journal of the American Statistical Association*, **62**, 500–9.

Pesaran, M.H. (2021) General diagnostic tests for cross section dependence in panels, *Empirical Economics*, **60**, 13–50.

Raftery, A.E., Currie, J., Bassett, M.T., and Groves, R. (2020). *Evaluating data types: A Guide for Decision Makers using Data to Understand the Extent and Spread of COVID-19*, The National Academies Press, Washington, DC.

Schuchat, A. (2020) Public health response to the initiation and spread of pandemic COVID-19 in the United States, February 24-April 21, 2020, *Morbidity and Mortality Weekly Report*, **69**, 551–6.

Singh, S., Shaikh, M., Hauck, K., and Miraldo, M. (2021) Impacts of introducing and lifting non-pharmaceutical interventions on COVID-19 daily growth rate and compliance in the United States, *Proceedings of the National Academy of Sciences United States of America*, **118**, 1–9.

Ward, M.P., Xiao, S., and Zhang, Z. (2020) Humidity is a consistent climatic factor contributing to SARS-CoV-2 transmission, *Transboundary and Emerging Diseases*, **67**, 3069–74.

Wooldridge, J.M. (2010). *Econometric Analysis of Cross Section and Panel Data*, 2nd edn, The MIT Press, Cambridge, MA.

Wu, Y., Jing, W., Liu, J., Ma, Q., Yuan, J., Wang, Y., Du, M., and Liu, M. (2020) Effects of temperature and humidity on the daily new cases and new deaths of COVID-19 in 166 countries, *The Science of the Total Environment*, **729**, 139051.